



## JOURNAL OF ENERGY, MATERIALS, AND INSTRUMENTATION TECHNOLOGY

Journal Webpage <https://jemit.fmipa.unila.ac.id/>



# Effect of Acid Hydrolysis on Preparation of Nanocellulose from *Swietenia mahagoni*

Rysa Sonya Reni Paulin Gultom\*, Posman Manurung, Pulung Karo Karo, Sri Wahyu Suciati, and Ayu Aprilia

Department of Physics, Faculty of Mathematics and Natural Sciences, University of Lampung, Bandar Lampung, Indonesia, 35141

### Article Information

#### Article history:

Received November 3, 2022

Received in revised form February 7, 2023

Accepted February 8, 2023

**Keywords:** Nanocellulose, hardwood, mahogany, acid hydrolysis

### Abstract

The extraction of the mahogany pulp as the main ingredient for the preparation of nanocellulose was carried out using the acid hydrolysis method. Sulfuric acid ( $H_2SO_4$ ) was used to hydrolyze the primary constituent and sodium hydroxide (NaOH) was utilized in the delignification process. The purpose of this study is to identify the properties of nanocellulose made from mahogany hardwood on fluctuations in  $H_2SO_4$  concentrations, particularly on concentration 19, 29, 39, and 45%. A Fourier Transform Infrared (FTIR) spectrophotometer, Scanning Electron Microscopy (SEM) and X-ray diffraction (XRD) were used to analyze the sample product, which is cellulose nanocrystal powder. The XRD results stated that the diameter of the nanocellulose crystal size ranged from 3-6 nm, while the SEM results showed that the sample's morphology resembled a stacked arrangement of stones. Meanwhile, the results of the FTIR indicated that the functional groups produced consisted of hydroxyl, aliphatic, aromatic rings, aryl carbonyls, and pyranose. Based on the tests, the best sample is obtained as a concentration variation of  $H_2SO_4$  39%, which produces a diameter of 3.6 nm with a crystallinity index as high as 80.48%.

### Informasi Artikel

#### Proses artikel:

Diterima 3 November 2022

Diterima dan direvisi dari 7 Februari 2023

Accepted 8 Februari 2023

**Kata kunci:** Nanoselulosa, kayu keras, mahoni, hidrolisis asam

### Abstrak

Telah dilakukan pembuatan nanoselulosa berbasis kayu mahoni dengan metode hidrolisis asam. Asam sulfat ( $H_2SO_4$ ) digunakan untuk menghidrolisis unsur utama dan Natrium hidroksida (NaOH) digunakan dalam proses delignifikasi. Tujuan dari penelitian ini adalah untuk mengetahui sifat nanoselulosa yang berasal dari kayu keras mahoni terhadap fluktuasi konsentrasi  $H_2SO_4$  khususnya pada konsentarsi 19, 29, 39, dan 45%. Spektrofotometer Fourier Transform Infrared (FTIR), Scanning Electron Microscopy (SEM), menggunakan X-Ray Diffraction (XRD) digunakan untuk menganalisis produk sampel, yaitu bubuk nanokristal selulosa. Hasil uji XRD menyatakan diameter ukuran kristal nanoselulosa berkisar antara 3-6 nm, sedangkan hasil uji SEM menunjukkan morfologi sampel yang menyerupai susunan batu yang bertumpuk. Sementara, hasil uji FTIR menyatakan gugus fungsi yang dihasilkan terdiri atas hidroksil, alifatik, cincin aromatik, karbonil aril, dan piranosa. Berdasarkan pengujian yang telah dilakukan, maka diperoleh hasil terbaik berupa variasi konsentrasi  $H_2SO_4$  39% yang menghasilkan diameter ukuran kristal sebesar 3,6 nm dengan derajat kristalinitas setinggi 80,48%.

## 1. Introduction

The primary building block of the cell walls of all organisms, from higher plants to bacteria, algae and flagellates, is cellulose (Fengel & Wegener, 1983). Cellulose is insoluble in various solvents and resistant to various chemical reactions, with the exception for strong acids generated by hydrogen bonds between hydroxyl groups in the cellulose chain (Karlsson, 2006). The formation of nanomaterials synthesized from natural cellulose materials through chemical hydrolysis methods can produce nanocellulose. The resulting nanocellulose exhibits high crystallinity, thermal stability and an average diameter of 10-25 nm (B. Deepa, 2015).

\* Corresponding author.

E-mail address: soniyagultom23@gmail.com

The application of nanocellulose in modern materials technology can be found in various fields, such as nanocomposites and biomedicine. Modified nanocellulose as a coating for composite materials can produce nanocomposites whose matrix is firmly bound and hydrophobic or waterproof (Hooshmand et al., 2014). Meanwhile, using nanocellulose in the medical field as an implant in the skeleton rehabilitates injured ligaments and tendons. The type of nanocellulose used is non-toxic, hydrophilic, has high strength, and is compatible with human organs (Mathew et al., 2012).

Different woods species, including *Acacia mangium* and mahang (*Macaranga gigantea*), have been explored for nanocellulose production (N. Bahar, 016). Hardwood is one of the basic materials derived from plants commonly used to manufacture nanocellulose. To determine the level of interest, nanocellulose can be graded based on its purity or crystallinity index. An example of nanocellulose extracted from *Eucalyptus spp.* and *Bixa spp.* Produce a sample with a crystallinity index as high as 76.00% (Lin et al., 2019). Another study extracted *Acacia caesia* into the form of nanocellulose that achieved a purity of 79.65% (Thomas et al., 2020).

Acid hydrolysis is a common method for producing nanocellulose from various biomass sources. The process parameters, such as acid type, concentration, temperature and reaction time, significantly influence the properties of the resulting nanocellulose (Mohammed Alhaji Mohammed, 2022). The extraction of nanocellulose is carried out using the acid hydrolysis method, which is preceded by the delignification process. Delignification using NaOH is used to release amorphous phases of the hardwood pulp. The amorphous phases include lignin and hemicellulose. Lignin is a three-dimensional network used to agglutinate cellulose cells and reinforce the structure of the wood. Meanwhile, hemicellulose is a non fibrous polysaccharide that is easy to swell with the function of an agglutinate single cell. These compounds cause the crystalline phase of cellulose to be trapped in the middle, so they must be removed through hydrolysis (Fratzl & Weinkamer, 2007). The hydrolysis process is a chemical reaction that deletes the amorphous region. Acid hydrolysis is a commonly used method for extracting nanocellulose (Nickerson & Habrle, 1947). The solution needed is sulfuric acid ( $H_2SO_4$ ), which is diluted in various concentrations. Using sulfuric acid can increase the dispersion of nanocellulose in aqueous solvents compared to other acid types, such as hydrochloric acid (Liu et al., 2014).

In this research, nanocellulose extracted from the mahogany pulp (*Swietenia mahagoni*), which was obtained from Pekalongan District, East Lampung Regency, with latitude and longitude of 5°5'54.845" S and 105°21'9.216" E. The reason for using mahogany in this research is to obtain the best sample purity and develop a primary material type from hardwoods in the local environment. The extraction step includes bleaching using NaClO, delignification, and hydrolysis. The chemical reaction can produce CNC (*Cellulose Nano Crystals*), which contain negatively charged sulfate groups, thereby increasing their dispersion in aqueous solvents (Liu et al., 2014). X-ray diffraction (XRD) and scanning electron microscopy (SEM) were used to investigate the crystallinity index, crystal size, cell characteristics and morphological structure of the extracted CNC powder.

## 2. Research Methods

The materials was used in this research are mahogany pulp, *Bayclin* textile bleach (5.25% NaClO), *Merck* 98% NaOH, *Merck* 98%  $H_2SO_4$ , distilled water (*aquades*) and double distilled water (*aquabides*).

First, the mahogany pulp was bleached using 5.25% NaClO and then dried in the sun. Then, 10 g of dry pulp was mixed with 100 ml of 3% NaOH and stirred at 50°C for 2 h. This stage is called delignification, which is the removal of lignin. After this stage, the precipitate contained is taken and mixed with 100 ml of  $H_2SO_4$  with various concentrations (19, 29, 39, and 45%) and then stirred while heating at 45°C in the open state for an hour. This acid hydrolysis step aims to remove the remaining hemicellulose and lignin with products in the form of pre-Cellulose Nano Crystals (p-CNC).

Next, p-CNC was washed using 300 ml *aquabides* and neutralized with 10% NaOH until it reached pH 7. Then, the sample was dialyzed by centrifugation for 10 min until three times. The p-CNC precipitate was filtered using filter paper and dried in an oven at 100°C for 30 min at regular intervals. The final product, which was in CNC form, was grounded with agate mortar.

The obtained CNC powder was then characterized by XRD and SEM. XRD characterization was performed at Glabs Indonesia Utama Bandung using the Rigaku Miniflex. The characterization results determined the crystallinity index, crystal size, and cell parameters. Meanwhile, SEM characterization was collected at FMIPA ITB using a Hitachi SU3500 instrument to obtain results in morphological displays of samples.

## 3. Results and Discussions

**Figure 1** shows the results of the synthesis of mahogany pulp through an acid hydrolysis process into CNC powder.

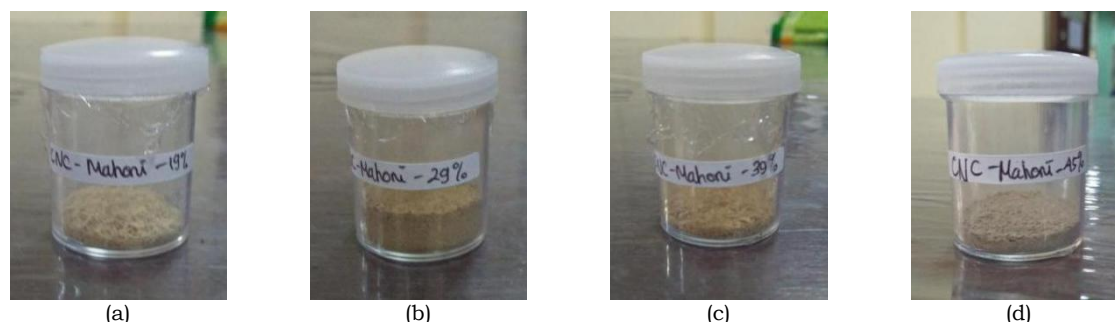


**Figure 1.** CNC resulting from the hydrolysis of  $H_2SO_4$  (a) 19%, (b) 29%, (c) 39%, and (d) 45%

Based on **Figure 1**, the increase of  $H_2SO_4$  caused the color of the sample to darken. It is due to the presence of  $H_2SO_4$  plus water, which produces heat. It is well known that acid solutions have strong oxidizing properties. As a

result, cellulose hydrolysis causes degradation, dehydration, and carbonization, which is the burning of cellulose carbon. This carbonation causes the color of the sample to darken (Ioelovich, 2012).

### 3.1 XRD Analysis

#### 1. Qualitative Analysis

**Figure 2** shows the XRD results of the four samples. Matching methods between database and XRD data carried out qualitative analysis. Crystallography Open Database (COD) of 4114994 and 4114382 for Ia and Ib, respectively (Nishiyama et al., 2002; 2003). Ia's crystalline phases are 15-16°, and Ib is 22-23° (Caballero et al., 2016).

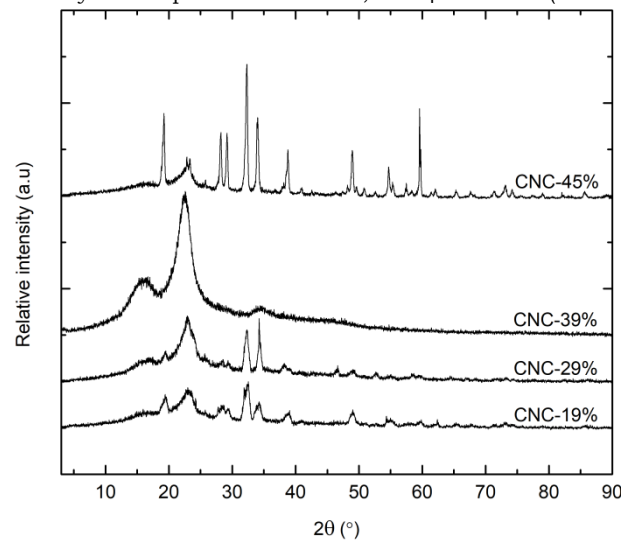


**Figure 2.** Diffractogram of nanocellulose in different sulfuric acids

Based on **Figure 2**, the diffractogram demonstrates that the CNC-39% sample has the sharpest and most distinct peaks compared to other samples. This peak clarity reflects a higher degree of structural order, affirming that CNC-39% has the highest crystallinity index among the tested concentrations. Then, the purest nanocellulose diffractogram was obtained for the CNC-39% sample, with the maximum peak at  $2\theta$  being 22.68°. Compared to the previous study, with the maximum peak in the range of 22.51°, there is a difference of 0.17° and a value shift of 0.38% (Khan et al., 2020). Because the value shift is under 1%, it can be assumed that the results agree with previous research.

To determine the level of CNC crystallinity, the calculations are based on Segal's formula (Segal et al., 1959):

$$I_c = \frac{I_{max} - I_{am}}{I_{max}} \times 100\% \quad (1)$$

whit  $I_c$  is a crystallinity index,  $I_{max}$  is the intensity of maximum diffraction peak, and  $I_{am}$  is the intensity of amorphous baseline. The crystallinity results after using **Equation 1** are shown in **Table 1**.

**Table 1.** CNC crystallinity index calculation results

Sample	$2\theta_{max}$ (°)	$I_{max}$ (cps)	$2\theta_{am}$ (°)	$I_{am}$ (cps)	$I_c$ (%)
CNC-19%	23.13	5986	18.94	1816.67	69.65
CNC-29%	22.99	7347	18.90	1908.33	74.03
CNC-39%	22.68	13877	18.68	2708.33	80.48
CNC-45%	23.34	1152	18.24	891.67	22.60

Based on **Table 1**, the highest crystallinity index is obtained in the sample CNC-39% of 80.48%. This number is higher than that of other nanocellulose processed from different woods. Nanocellulose extracted from a mixture of *Eucalyptus spp.* and *Bixa spp.* has a crystallinity index of 76.00 (Lin et al., 2019). On the other hand, nanocellulose extracted from *Acacia caesia* has a crystallinity index of 79.65% (Thomas et al., 2020). The last research was prepared from *Swietenia mahagoni*, which produced 80.48% purity of the sample, indicating that the same method but different ingredients caused the various crystallinity indexes of the nanocellulose. The best crystallinity index can be obtained by extracting other hardwood materials from the local environment. However, there is a degradation of crystallinity index on a sample extracted with  $H_2SO_4$  45%, where the percentage decreased from 80.48 to 22.60%. The degradation is caused by increased  $H_2SO_4$  concentration used in the extracted process, up to 39%. So, a limit of acid concentration can extract cellulose into nanosized.

To calculate the crystal size of nanocellulose, the Scherrer's formula is used which is written as (Cullity, 1978):

$$L = \frac{K \lambda}{B \cos \theta} \quad (2)$$

where  $L$  is the diameter of crystal size in the nanoscale (nm),  $K$  is a Scherrer's constant of 0.94, and  $\lambda$  is the X-ray wavelength.  $B$  is determined as the full width at half maximum (FWHM), and  $\theta$  is the angle of the diffraction peak.

The calculation results of crystal size based on XRD data sequentially are 3.1, 3.4, 3.6, and 5.7 nm, as shown in **Figure 4**.

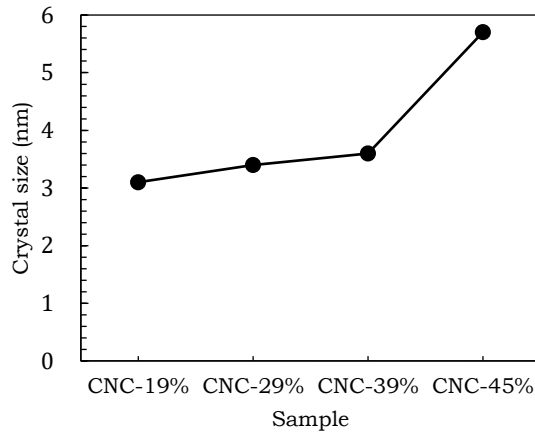


**Figure 4.** CNC diameter of crystal size

The crystal size of CNC increases with increasing sulfuric acid concentration. The crystal size of CNC-39% is 3.60 nm so that it can be classified as hardwood nanocellulose with a diameter size range of 3–35 nm (Gopi et al., 2019; Khan et al., 2020; Liimatainen et al., 2013).

## 2. Quantitative Analysis

Quantitative analysis was performed by refining the XRD data using Rietica software. Because of the database limitation, the calculation method used is Le bail. In this analysis, the cell parameters used are Nishiyama et al. (2002; 2003) for nanocellulose of  $I\alpha$  and  $I\beta$ . Meanwhile, those samples that contain additives of impurities were used Ferreira's (COD: 2007312) for lignin and Hawthorne's for thenardite (COD: 9004092) (Ferreira et al., 1998; Hawthorne & Ferguson, 1975). The results of data refinement are shown in **Figure 3**.

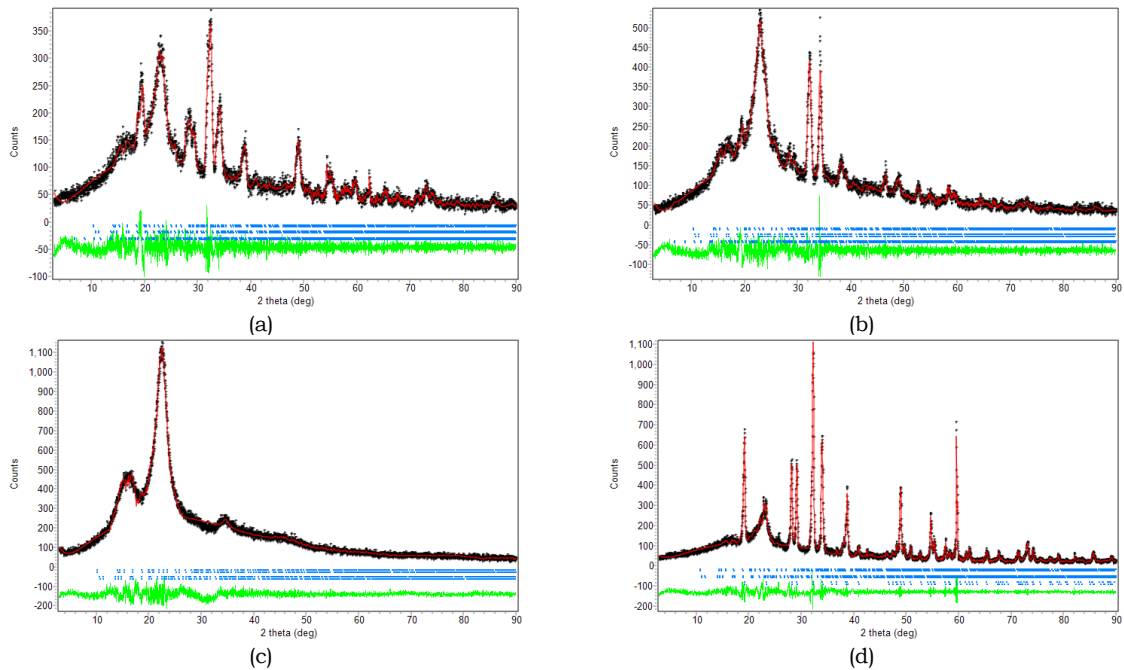


**Figure 3.** XRD data refinement results (a) CNC-19%, (b) CNC-29%, (c) CNC-39%, and (d) CNC-45%

Based on **Figure 3**, only the sample of CNC-39% contains two phases of  $I\alpha$  and  $I\beta$ . CNC-19% and CNC-29% contain an additional phase in lignin (Ferreira et al., 1998), while CNC-45% contains thenardite (Hawthorne & Ferguson, 1975). These can be explained through the data in **Table 2**.

**Table 2.** CNC phase parameters in molar percent (%M)

Sample	I $\alpha$ (%M)	I $\beta$ (%M)	Lignin (%M)	Thenardite (%M)
CNC-19%	3.75 $\pm$ 0.00	14.81 $\pm$ 0.00	81.44 $\pm$ 0.02	-
CNC-29%	3.73 $\pm$ 0.00	14.87 $\pm$ 0.00	81.41 $\pm$ 0.02	-
CNC-39%	19.98 $\pm$ 0.03	80.02 $\pm$ 0.09	-	-
CNC-45%	4.55 $\pm$ 0.00	17.95 $\pm$ 0.00	-	77.50 $\pm$ 0.01

**Table 2** shows the molar percentage of phases contained in each sample. Acid concentrations that are too low cannot completely dissolve the amorphous phase of lignin. Meanwhile, the highest concentration will give rise to a new crystalline phase of thenardite. The CNC-39% sample contains only two phases of crystalline cellulose in form I $\alpha$  and I $\beta$ , which shows the accuracy of the diffractogram in **Figure 2**. The molar percentage of I $\beta$  is approximately four times that of I $\alpha$ , which proves the degradation of I $\alpha$  to I $\beta$  through hydrolysis (Wada & Okano, 2001).

To find out that the diffractogram refinement of the CNC-39% sample produces cell parameters that correspond to the Nishiyama models, the calculation of the value shift or relative error is shown in **Table 3-4**.

**Table 3.** I $\alpha$  phase cell parameters

Sample	a (Å)	b (Å)	c (Å)	$\alpha$ (°)	$\beta$ (°)	$\gamma$ (°)
Model	6.717	5.962	10.400	118.08	114.80	80.37
CNC-39%	6.648	5.886	10.449	117.94	114.71	80.43
RE (%)	0.516	0.641	0.235	0.06	0.04	0.04

**Table 4.** I $\beta$  phase cell parameters

Sample	a (Å)	b (Å)	c (Å)	$\alpha$ (°)	$\beta$ (°)
Model	7.784	8.201	10.380	90.00	96.50
CNC-39%	7.742	8.206	10.403	90.00	96.47
RE (%)	0.271	0.030	0.111	0.00	0.02

**Table 3-4** shows the results of calculating the relative error (RE) between the cell parameters of the I $\alpha$  and I $\beta$  phase model with a sample CNC of 39%. All RE values are below 1%, indicating that CNC-39% cell parameter values follow Nishiyama et al.'s model (2002; 2003).

### 3.2 SEM Analysis

SEM characterization was used to determine the appearance of the CNC-39% sample's nanostructure morphology, as illustrated **Figure 5**.

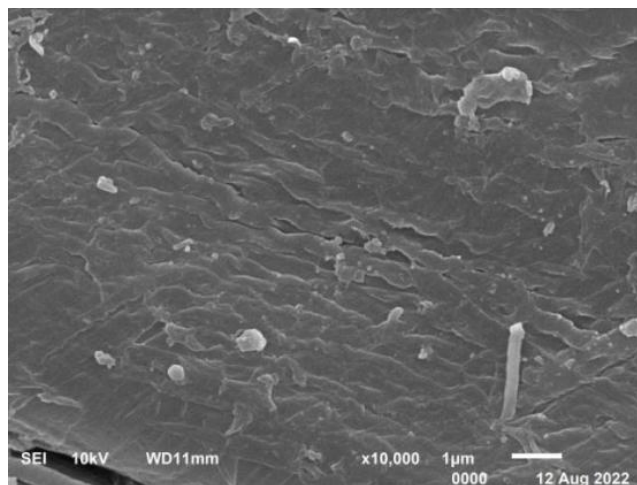


**Figure 5.** SEM observation of sample CNC-39%

Based on **Figure 5**, CNC-39 %'s morphology has an overlapping structure resembling a compact rock slab. It leads to phase I $\alpha$  and I $\beta$  particles being indistinguishable from each other. In addition, agglomeration is caused by an increase in concentration of H<sub>2</sub>SO<sub>4</sub>, which increases the temperature. This incorporation also causes an increase in crystal size as the acid concentration increases (Rosanti et al., 2020).

### 3.3 FTIR Analysis

FTIR characterization was conducted to identify the samples' functional groups, and the results are presented in **Figure 6**.



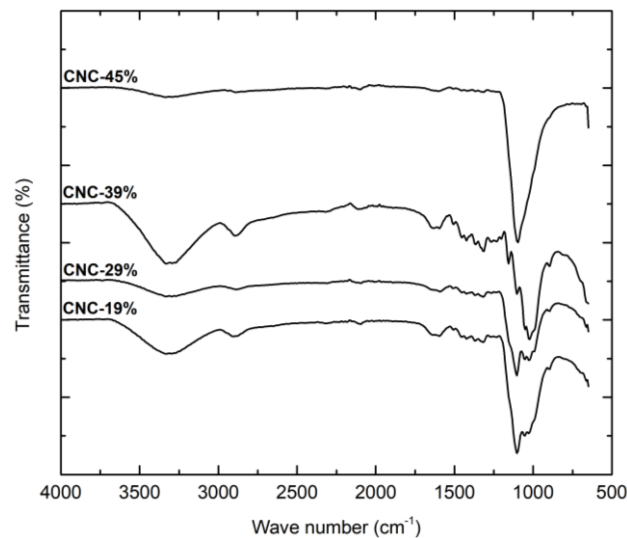


**Figure 6.** FTIR spectra of CNC samples

**Figure 6** shows the spectra of the CNC-39% sample, which have the sharpest absorption regions among the others, which are determined by the low transmittance value. Because the transmittance value is the opposite of the absorption value, it indicates that a particular wave number has many functional groups detected (Nandiyanto et al., 2019). The names of the functional groups detected are shown in **Table 5** (Libretexts, 2022).

**Table 5.** *B* phase cell parameters

Wave number (cm <sup>-1</sup> )				Functional groups		References
CNC-19%	CNC-29%	CNC-39%	CNC-45%			
3332.2	3332.2	3332.2	3339.7	O-H	Hydroxyl	(Mo et al., 2009)
2899.9	2885.0	2892.4	2892.4	C-H	Aliphatic	(Sain & Panthapulakkal, 2006)
2102.2	-	2109.7	-	C≡C	Alkyne	(Coates, 2000)
-	2094.8	-	-	N=C=S	Isothiocyanate	(Coates, 2000)
1595.3	1595.3	1595.3	1602.8	C=C	Aromatic ring	(Yang et al., 2021)
1423.8	1423.8	1423.8	-	H-C-H	Methylene	(Jonoobi et al., 2009)
1319.5	1319.5	1312.0	1319.5	C-O	Aryl carbonyl	(Yang et al., 2021)
1103.3	1103.3	1028.7	1103.3	C-O-C	Pyranose	(Rampengan, 2017)
-	1028.7	-	-	C-O-C	Pyranose	(Rampengan, 2017)

**Table 5** shows that five functional groups will always be in the sample. The hydroxyl group indicates the strong interaction between cellulose and water molecules (Johar et al., 2012), while the aliphatic is part of lignocellulose (Sain & Panthapulakkal, 2006). The following detected groups are the aromatic ring and aryl carbonyl from the lignin compound (Yang et al., 2021). Meanwhile, pyranose is the last detected group that indicates the increase of crystallinity of nanocellulose (Rampengan, 2017).

#### 4. Conclusions

The preparation of nanocellulose has been successfully extracted from *Swietenia mahagoni* pulp. Nanocellulose extracted from mahogany has a crystal diameter of 3-6 nm. The best sample was extracted with H<sub>2</sub>SO<sub>4</sub> 39%, with a crystal diameter of 3.6 nm and a crystallinity index of 80.48%. This high crystallinity value is also determined by the existence of the pyranose group from FTIR analysis. The increase of sulfuric acid concentration can accelerate the degradation of phase *I*<sub>α</sub>, which becomes *B* and increases the size of cellulose nanocrystal.

#### 5. Acknowledgment

The author thanks Sri Wahyu Suciayati for helping funding for this research.

#### 6. Bibliography

- Alhaji Mohammed, M., Basirun, W.J., Abd Rahman, N.M., Shalauddin, M., & Salleh, N.M. (2022). The Effect of Acid Hydrolysis Parameters on the Properties of Nanocellulose Extracted from Almond Shells. *Journal of Natural Fibers*, 19, 14102 - 14114.
- Bahar, N., Hidayat, T., Elyani, N., & Rostika, I. (2013). The Potential of Nanocellulose from *Acacia Mangium* Pulp for Specialty Paper Making. *Jurnal Selulosa* Vol 3, No 1.
- Caballero, B., Finglas, P. M., & Toldra, F. (2016). *Encyclopedia of Food and Health*. Amsterdam: Elsevier Ltd.
- Coates, J. (2000). Interpretation of Infrared Spectra, A Practical Approach. *Encyclopedia of Analytical Chemistry*, 8, 14.

- Cullity, B. (1978). *Elements of X-ray Diffraction, Second Edition*. Boston: Adision Wesley Publishing Company Inc.
- Deepa, B., Abraham, E., Cordeiro, N., Mozetič, M., Mathew, A.P., Oksman, K., Faria, M., Thomas, S., & Pothan, L.A. (2015). Utilization of various lignocellulosic biomass for the production of nanocellulose: a comparative study. *Cellulose*, 22, 1075-1090.
- Fengel, D., & Wegener, G. (1983). *Wood: Chemistry, Ultrastructure, Reactions*. Berlin: Walter de Gruyter.
- Ferreira, M. A., Costa, M. D. D., Mendes, I. M. C., Drumond, M. G., Pilo-Veloso, D., & Fernandes, N. G. (1998). Lignin Model Compounds: 4,4'-O-Dimethyldehydrodiacetovanilloee and 4,4'-O-Diethyldehydrodiacetovanilloee. *Acta Crystallographica Section C*, 54(6), 837-838. <https://doi.org/10.1107/S0108270197018015>
- Fratzl, P., & Weinkamer, R. (2007). Nature's Hierarchical Materials. *Progress in Material Science*, 52(8), 1267-1270. <https://doi.org/10.1016/j.pmatsci.2007.06.001>
- Gopi, S., Balakrishnan, P., Chandradhara, D., Poovathankandy, D., & Thomas, S. (2019). General Scenarios of Cellulose and Its Use in The Biomedical Field. *Mater. Today Chem.*, 13, 59-78. <https://doi.org/10.1016/j.mtchem.2019.04.012>
- Hawthorne, F. C., & Ferguson, R. B. (1975). Anhydrous Sulfates I: Refinement of The Crystal Structure of Celestite with An Appendix on The Structure of Thenardite. *Can. Mineral.*, 13(2), 181-187.
- Hooshmand, S., Aitomaki, Y., Skrifvars, M., Mathew, A. P., & Oksman, K. (2014). All-Cellulose Nanocomposite Fibers Produced by Melt Spinning Cellulose Acetate Butyrate and Cellulose Nanocrystals. *Cellulose*, 21(4), 2665-2678. <https://doi.org/10.1007/s10570-014-0269-4>
- Ioelovich, M. (2012). Optimal Conditions for Isolation of Nanocrystalline Cellulose Particles. *Nanoscience and Nanotechnology*, 2(2), 9-13. <https://doi.org/10.5923/j.nn.20120202.03>
- Johar, N., Ahmad, I., & Dufresne, A. (2012). Extraction, Preparation, and Characterization of Cellulose Fibres and Nanocrystals from Rice Husk. *Industrial Crops and Products*, 37(1), 93-99. <https://doi.org/10.1016/j.indcrop.2011.12.016>
- Jonoobi, M., Harun, J., Shakeri, A., Misra, M., & Oksman, K. (2009). Chemical Composition, Crystallinity, and Thermal Degradation of Bleached and Unbleached Kenaf Bast (*Hibiscus cannabinus*) Pulp and Nanofibers. *BioResources*, pp. 4, 633-634.
- Karlsson, H. (2006). *Fibre Guide: Fibre Analysis and Process Applications in The Pulp and Paper Industry*. Swedia: AB Lorentzen and Wettre.
- Khan, M. N., Rehman, N., Sharif, A., Ahmed, E., Farooqi, Z. H., & Din, M. I. (2020). Environmentally Benign Extraction of Cellulose from Dunchi Fiber for Nanocellulose Fabrication. *International Journal of Biological Macromolecules*, 153, 74-75. <https://doi.org/10.1016/j.ijbiomac.2020.02.333>
- Libretexts. (2022). *Infrared Spectroscopy Absorption Table*. Retrieved from <https://chem.libretexts.org/@go/page/22645>
- Liimatainen, H., Visanko, M., Sirvio, J., Hormi, O., & Niinimäki, J. (2013). Sulfonated Cellulose Nanofibrils Obtained from Wood Pulp through Regioselective Oxidative Bisulfite Pre-treatment. *Cellulose*, 20(2), 741-749. <https://doi.org/10.1007/s10570-013-9865-y>
- Lin, K., Enomae, T., & Chang, F. (2019). Cellulose Nanocrystal Isolation from Hardwood Pulp Using Various Hydrolysis Conditions. *Molecules*, 24(3724), 1-15.
- Liu, P., Sehaqui, H., Tingaut, P., Wichser, A., Oksman, K., & Mathew, A. P. (2014). Cellulose and Chitin Nanomaterials for Capturing Silver Ions (Ag<sup>+</sup>) from Water via Surface Adsorption. *Cellulose*, 21, 449-461. <https://doi.org/10.1007/s10570-013-0139-5>
- Mathew, A. P., Oksman, K., Pierron, D., & Harmand, M. (2012). Fibrous Cellulose Nanocomposite Scaffolds Prepared by Partial Dissolution for Potential Use as Ligament or Tendon Substitutes. *Carbohydrate Polymers*, pp. 87, 2291-2298. <https://doi.org/10.1016/j.carbpol.2011.10.063>
- Mo, Z., Zhao, Z., Chen, H., Niu, G., & Shi, H. (2009). Heterogeneous Preparation of Cellulose-Polyaniline Conductive Composites with Cellulose Activated by Acids and Its Electrical Properties. *Carbohydrate Polymers*, 75(4), 661. <https://doi.org/10.1016/j.carbpol.2008.09.010>
- Nandiyanto, A. B. D., Oktiani, R., & Ragadhita, R. (2019). How to Read and Interpret FTIR Spectroscopy of Organic Material. *Indonesian Journal of Science and Technology*, 4(1), 97-118.

---

<https://doi.org/10.17509/ijost.v4i1.15806>

- Nickerson, R. F., & Habrle, J. A. (1947). Cellulose Intercrystalline Structure: Study by Hydrolytic Methods. *Journal of Industrial and Engineering Chemistry*, 39(11), 1507–1512.
- Nishiyama, Y., Langan, P., & Chanzy, H. (2002). Crystal Structure and Hydrogen-Bonding System in Cellulose I $\beta$  from Synchrotron X-ray and Neutron Fiber Diffraction. *American Chemical Society*, 125(31), 9076.
- Nishiyama, Y., Sugiyama, J., Chanzy, H., & Langan, P. (2003). Crystal Structure and Hydrogen Bonding System in Cellulose Ia from Synchrotron X-ray and Neutron Fiber Diffraction. *American Chemical Society*, 125(47), 14301.
- Rampengan, A. M. (2017). Analisis Gugus Fungsi pada Polimer Polyethylene Glycol (PEG) Coated-Nanopartikel Oksida Besi Hitam (Fe<sub>3</sub>O<sub>4</sub>) dan Biomolekul. *Fullerene Journal of Chemistry*, 2(2), 97.
- Rosanti, A. D., Wardani, A. R. K., & Anggraeni, H. A. (2020). Pengaruh Suhu Kalsinasi terhadap Karakteristik dan Aktivitas Fotokatalis N/TiO<sub>2</sub> pada Penjernihan Limbah Batik Tenun Ikat Kediri. *Cakra Kimia*, 8(1), 30.
- Sain, M., & Panthapulakkal, S. (2006). Bioprocess Preparation of Wheat Straw Fibers and Their Characterization. *Industrial Crops and Products*, 23, 5. <https://doi.org/10.1016/j.indcrop.2005.01.006>
- Segal, L., Creely, J. J., Martin, A. E. J., & Conrad, C. M. (1959). An Empirical Method for Estimating the Degree of Crystallinity of Native Cellulose Using the X-Ray Diffractometer. *Textile Research Journal*, 29(10), 786–794.
- Thomas, S., Begum, P. M. S., Dominic, C. D., Salim, N. V., Hameed, N., Rangappa, S. M., ... Parameswaranpillai, J. (2020). Isolation and Characterization of Cellulose Nanowhiskers from Acacia caesia Plant. *Journal of Applied Polymer*, 1–9. <https://doi.org/10.1002/app.50213>
- Wada, M., & Okano, T. (2001). Localization of Ia and I $\beta$  Phases in Algal Cellulose Revealed by Acid Treatments. *Cellulose*, 8(3), 183–188.
- Yang, T., Liu, P., Xu, D., Wang, J., & Zhang, K. (2021). Direct Preparation of Nanocelluloses of Tunable Lengths from Native Wood Via Alkaline Periodate Oxidation. *Nanomaterials*, 2100058, 3–4. <https://doi.org/10.1002/adsu.202100058>